Carbohydrate Research 344 (2009) 985–995

Contents lists available at ScienceDirect

Carbohydrate Research

journal homepage: www.elsevier.com/locate/carres

Physicochemical features of ultra-high viscosity alginates

Henning Storz [a], Kilian J. Müller [b], Friederike Ehrhart [c], Ivan Gómez [d], Stephen G. Shirley [c], Petra Gessner [b], Gertraud Zimmermann [b], Esther Weyand [e], Vladimir L. Sukhorukov [b], Thomas Forst [f], Matthias M. Weber [e], Heiko Zimmermann [c], Werner-Michael Kulicke [a], Ulrich Zimmermann [b,*]

[a] Institute for Technical and Macromolecular Chemistry, University of Hamburg, Bundesstrasse 45, 20146 Hamburg, Germany
[b] Lehrstuhl für Biotechnologie, Biozentrum, University of Würzburg, Am Hubland, 97074 Würzburg, Germany
[c] Abteilung Biophysik & Kryotechnologie, Fraunhofer-Institut für Biomedizinische Technik IBMT, Ensheimer Straße 48, 66386 St. Ingbert, Germany
[d] Universidad Austral de Chile, Instituto de Biologia Marina, Facultad de Ciencias, Casilla 567, Valdivia, Chile
[e] Schwerpunkt Endokrinologie und Stoffwechselerkrankungen, Medizinische Klinik und Poliklinik, Universitätsklinik Mainz, 55131 Mainz, Germany
[f] Institute for Clinical Research and Development, Parcusstraße 8, 55116 Mainz, Germany

ARTICLE INFO

Article history:
Received 24 November 2008
Received in revised form 18 February 2009
Accepted 19 February 2009
Available online 25 February 2009

Keywords:
Ultra-high viscosity alginates
Intrinsic viscosity
Molar mass distribution
Coil size
Guluronate
Multi-angle light scattering

ABSTRACT

The physicochemical characteristics of the ultra-high viscosity and highly biocompatible alginates extracted from *Lessonia nigrescens* (UHV_N) and *Lessonia trabeculata* (UHV_T) were analyzed. Fluorescence and ^1H NMR spectroscopies, viscometry, and multi-angle light scattering (MALS) were used for elucidation of the chemical structure, molar mass, and coil size. The sequential structures from NMR spectroscopy showed high guluronate content for UHV_T, but low for UHV_N. Intrinsic viscosity $[\eta]$ measurements exhibited unusual high values (up to 2750 mL/g), whereas $[\eta]$ of a commercial alginate was only about 970 mL/g. MALS batch measurements of the UHV-alginates yielded ultra-high values of the weight average molar mass (M_w up to 1.1×10^6 g/mol) and of the *z*-average gyration radius ($\langle R_G \rangle_z$ up to191 nm). The M_w and $\langle R_G \rangle_z$ distributions of UHV-alginates and of ultrasonically degraded fractions were determined using size exclusion chromatography combined with MALS and asymmetrical flow-field-flow fractionation. The M_w dependency of $[\eta]$ and $\langle R_G \rangle_z$ could be described by $[\eta] = 0.059 \times M_w^{0.78}$ and $\langle R_G \rangle_z = 0.103 \times M_w^x$. ($UHV_N$: $x = 0.52$; UHV_T: $x = 0.53$) indicating that the monomer composition has no effect on coil expansion. Therefore, the equations can be used to calculate M_w and $\langle R_G \rangle_z$ values of UHV_T- and UHV_N-alginate mixtures as used in immunoisolation. Furthermore, the simple and inexpensive capillary viscometry can be used for real-time validation of the extraction and purification process of the UHV-alginates.

1. Introduction

Transplantation of immunoisolated human (or animal) therapeutic cells or tissues to treat human disorders promises to overcome some limitations of current therapies. Encapsulation protects the cells against the immune response of the host, avoids a lifetime of immunosuppressive therapy, and permits the moment-to-moment fine regulation of the missing therapeutic factor.[1] Among the numerous natural and synthetic polymers proposed for cell encapsulation, alginate has been and will probably continue to be one of the most commonly used biomaterials. Alginic acids and their salts have unique physicochemical properties, useful gelling properties in the presence of multivalent cations, and can retain a significant amount of water.[2–4] These features also render them useful for a wide range of other biomedical applications (e.g., cell therapy of cartilage, cryoprotection, wound dressings, and design of smart drug delivery systems).[5–14]

Alginates are linear anionic polysaccharides. The 1,4-linked α-L-guluronate and β-D-mannuronate are arranged in homopolymeric (GG and MM) blocks interspersed with blocks of alternating structures (MG) (Fig. 1). The results obtained by Ca^{2+} gelling of low-viscosity commercial alginates suggest that guluronate blocks are preferentially involved in selective binding of the divalent cations that induce chain–chain association.[15–17]

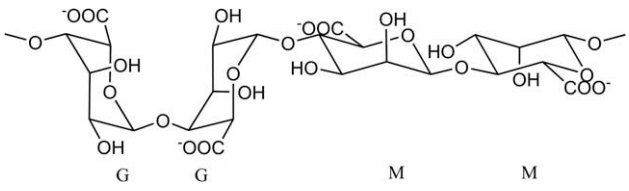

Figure 1. Schematic representation of the sequential block structure of alginates. The fragment: GGMM (G = guluronic acid; M = mannuronic acid) is shown. Note that the ratio of the fractions of the blocks (dyads) GG, MM, GM, and MG depends on the algal input source.

* Corresponding author. Tel.: +49 931 8884508; fax: +49 931 8884509.
E-mail address: zimmermann@biozentrum.uni-wuerzburg.de (U. Zimmermann).

0008-6215/$ - see front matter © 2009 Elsevier Ltd. All rights reserved.
doi:10.1016/j.carres.2009.02.016

Alginates are mainly extracted from brown seaweed. Input sources for commercial alginates are dried algal material washed ashore by the surf and the wind. This material is polluted with components of bacterial, fungal, animal, and anthropogenic origin evoking immunogenic reactions upon transplantation. Exposure of the washed up material to UV irradiation and high temperatures leads to degradation of polymer length. This is disadvantageous because biocompatibility of encapsulation material increases with increasing molar mass.[18] Furthermore, blended material is used in the commercial production of alginate. However, the M:G ratio as well as the size and distribution of the individual MG-blocks differs considerably among brown algae species. Information about impurities as well as M:G composition, sequential structure, and polymer length are not given by manufacturers even though these parameters dictate the physicochemical, gelling, and immunological properties of the alginates.[12]

Alginates of uniform composition, polymeric structure, and extremely high molecular mass (i.e., ultra-high viscosity) can be obtained if stipes of brown algae are used as sole input. As shown by experiments over nine years the quality of the stipes and thus the molecular properties of the alginate were quite reproducible provided that the stipes were harvested directly from the sea and processed immediately. Furthermore, contamination of the final alginate product by inorganic and organic impurities (including spores of gram-positive and gram-negative bacteria) is considerably reduced if the outer cell wall is removed, followed by treatment of the peeled stipe pieces with antimicrobial agents and with O_2-plasma before they are subjected to alginate extraction.[4,12] Transplantation of rat and human islets encapsulated in purified, ultra-high viscosity alginates cross-linked with Ba^{2+} into immuno-incompetent mice with chemically induced diabetes has led to normoglycemia for nearly one year.[19]

These results and work in the last few years have shown that a 1:1 mixture of ultra-high viscosity alginates extracted from *Lessonia nigrescens* and *Lessonia trabeculata* results in formulation of microcapsules which meet the stringent transplantation demands of biocompatibility, stability, elasticity, and permeability.[2,3,12] *L. nigrescens* grows in the tidal zone of the Chilean coast and is exposed to extremely high surf. The stipes are very elastic and flexible due to a relatively high amount of mannuronate. By contrast, *L. trabeculata* inhabits the rocky subtidal zone along the coast of central and northern Chile. The stipes of this species contain large amounts of guluronate and are therefore very stiff. The morphology, reproduction, growth, photosynthetic activity, and distribution of these two species have been extensively investigated in the last two decades.[20–26] However, practically nothing is known about the physicochemical and the related immunological properties of the alginates extracted from the two species. Data on this subject matter are urgently required for finalization of the standard operation procedures (SOPs) and other regulatory requirements.

This study was initiated to extend our knowledge about the physicochemical features of ultra-high viscosity alginates extracted from *L. nigrescens* and *L. trabeculata*. Main objectives were to quantify their purity and to reveal their structure–property relationships. These studies together with comparative measurements on commercial low viscosity alginates (which are usually used for immunoisolated transplantation) showed that the ultra-high viscosity alginates represent a novel class of compounds.

2. Experimental

2.1. Alginates

Stipes of *L. trabeculata* and *L. nigrescens* were used as starting material for the production of ultra-high viscosity alginates of clinical grade (denoted UHV_T- and UHV_N-alginates, respectively). Stipes were collected close to Coquimbo, Chile. Only fresh stipes that were free of epiphyte overgrowth were used. Immediately after harvesting from the sea, the stipes were subjected to antimicrobial treatment and the outer (approximately 1–2 mm thick) cell wall layer was completely removed. In addition, infection sites that could obviously be traced back to herbivory were cut out. Then the stipes were washed, cut into small pieces, and dried at 50 °C in a drying cabinet. Dried material was vacuum-sealed. Before use, the dried stipe pieces were treated with O_2-plasma. This treatment removes most immunogenic bacterial and animal debris from the surface of the peeled stipes (for details, see Zimmermann et al.[12]). Alginate extraction and purification used a 70 l bioreactor (see Zimmermann et al.[12]). Briefly, EDTA was used for the extraction of alginate from *L. trabeculata*, whereas the alginate from *L. nigrescens* was extracted by imino-disuccinate. For complete extraction it was necessary to pre-treat the stipe pieces with ice-cold HCl. After extraction, the solution was filtered and the alginate precipitated with ethanol (37.5% v/v) under injection of air. The precipitate was dissolved in 0.5 M KCl solution and subjected to two more ethanol precipitation steps. The entire process was performed at room temperature to avoid degradation of the polymeric chains. Finally, the white precipitate was sterilized with ethanol, dried under sterile conditions, and stored at 4 °C.

For control experiments, the commercial LV-alginate Manugel GHB (NutraSweet Kelco, Giran, UK) used in many immumoisolated transplantation studies was also investigated without any further purification.

For physicochemical characterization, the alginates were dissolved in saline solution consisting of ultrapure water from a Millipore Synergy water system (Millipore GmbH, Schwalbach, Germany) and containing 0.151 mol/mL NaCl and 200 ppm sodium azide (in order to prevent bacterial growth; PA grade; Merck, Darmstadt, Germany); the final sodium concentration was 0.154 mol/mL (so-called reference solvent).

2.2. Determination of the dry weight of UHV-alginates

The dry weight of the alginate samples was determined using a thermogravimetric analyzer (409C/MS, NETZSCH, Selb, Germany). The heating rate was 5 °C/min within a temperature range from 20 to 350 °C.

2.3. Determination of inorganic and organic impurities

The concentration of metal ions in the purified UHV_T- and UHV_N-alginate samples was determined using Inductively Coupled Plasma Optical Emission Spectrometry (ICP-OES; JY 70 Plus ICP-spectrometer, Instruments S.A., Longjumeau, France). The chloride content was determined by ion chromatography using an ion chromatograph (2000-I; exchange column AS14, both Dionex, Idstein, Germany).

The concentrations of polyphenol-like compounds and protein contaminants in the alginate samples were determined by fluorescence spectroscopy (excitation/emission: polyphenol-like compounds 366 nm/380–550 nm; proteins 270 nm/300–500 nm; see Leinfelder et al.[27]). Measurements were performed using an LS50 luminescence spectrometer (Perkin Elmer, Beaconsfield, UK). Contamination of purified UHV_T- and UHV_N-alginate with endotoxin (i.e., lipopolysaccharides being an integral part of the outer membrane of most gram-negative bacteria) was determined using the limulus-lysate assay. Assays were performed by ACILA AG, Mörfelden-Walldorf, Germany. The spatial distribution of phlorotannins (polymers of phloroglucinol; 1,3,5-trihydroxybenzene, i.e., a type of phenolic compounds found exclusively in brown algae) within the stipes was investigated by light microscopy after vanillin-HCl

staining.[28] The phlorotannin concentration was determined using the Folin–Ciocalteu reagent according to a modified method described by Koivikko et al.[29] For the determination of soluble phlorotannins, 100 mg dried algal material was macerated with liquid N_2 in a mortar and solubilized with 10 mL 70% acetone. The extracts were kept shaking overnight at 4 °C. After centrifugation, 500 mL of supernatant was mixed with 2.5 mL distilled water, 2 mL 20% $NaCO_3$, and 1 mL of 2 N Folin–Ciocalteu reagent. The samples were then incubated in darkness for 45 min at room temperature, centrifuged at 1878*g* (3 min), and the absorbance read at 730 nm. The insoluble (i.e., the cell-wall-bound fraction) phlorotannins were quantified using a modified alkaline method.[30] The precipitate from the first extraction was successively extracted using a solvent gradient: methanol, H_2O, methanol, acetone, and diethyl-ether. After drying of the extracts at 60 °C for 1 h, the total insoluble residue was re-suspended in 8 mL of 1 M aqueous NaOH solution (80 °C) and stirred for 2.5 h at room temperature. Samples were centrifuged (5 min at 2400*g*) and 1 mL aliquots were neutralized with 100 µl of H_3PO_4; the remaining NaOH was discarded. The alkaline treatment was repeated four times. Aliquots of each treatment were analyzed separately.

2.4. Immunogenicity of cross-linked alginates

To assess the in vivo biocompatibility, empty Ba^{2+} cross-linked alginate microcapsules were implanted by intraperitoneal injection into 5–6-week old Balb/c mice (n = 15). Alginate droplets produced by an air-jet droplet generator were cross-linked with external and internal Ba^{2+} as described by Zimmermann et al.[31] External gelling occurred upon contact of the droplets with a 20 mM $BaCl_2$ solution. The osmolality of the cross-linking solution was adjusted to 290 mOsm by appropriate amounts of NaCl; the pH was buffered at the physiological pH using 5 mM histidine. Internal gelling was achieved using the crystal gun method introduced by Zimmermann et al.[11,12,31] Dried and sterilized $BaCl_2$ crystals were driven by air pressure into the alginate droplets before they reached the cross-linking solution. The pressure of the crystal stream was adjusted to 1 bar. $BaCl_2$ crystals purchased from various suppliers were very heterogeneous. More homogeneous size and shape distributions were obtained by recrystallization. To this end, the commercially available crystals were dissolved in distilled water at 60 °C. Nanocrystals of $BaSO_4$ (diameter 10 nm, 0.53% w/v; Nanogate, Saarbrücken, Germany) were added as seed crystals to the supersaturated solution before cooling to 4 °C. The crystals were isolated by vacuum filtration, dried at 160 °C, and milled using a ceramic mortar with pestle (VWR, Darmstadt, Germany). A homogeneous size distribution (diameter 60–80 µm) was obtained by subsequent filtration through sieves of 63 µm and 90 µm pore diameter.

Microcapsules were counted and their size and volume determined before transplantation under sterile conditions. Control animals received the same volume of 0.154 mol/mL NaCl solution (n = 5). Microcapsules were retrieved 5 weeks after transplantation by examining the abdomen of the animals. Capsules were explanted by repeated flushes with warm 0.154 mol/mL NaCl solution containing 20 mM $BaCl_2$. Explanted microcapsules were evaluated for size, volume, and fibrotic overgrowth under a Wilowert S microscope (Hund GmbH, Wetzlar, Germany).

2.5. Ultrasonic degradation of alginates

For establishment of structure–property relationships (e.g., the [η]–M-relationship, see below) homologue series of UHV-alginate fractions were prepared by ultrasonic treatment. Unlike other degradation methods,[32–34] ultrasonic degradation has the advantage that the polymer chains break near their center of mass so no monomers or side chain reactions occur during the degradation process.[35–37] This leads to narrow distributed fractions with identical chemical composition.

UHV-alginates were dissolved in the reference solvent (0.7% w/v). 10 mL aliquots of the alginate solution were cooled to 4 °C and then subjected to sonication at a constant frequency of 20 kHz for up to 15 min using a Sonifier Cell Disruptor B15 (Branson, Danbury, CT, USA). In order to remove metal fines abraded from the tip of the resonator, the solutions were centrifuged at 15,000*g* for 30 min prior to the following determinations.

Because of the high viscosity, especially of UHV-alginates, NMR spectroscopy was performed on ultrasonically treated alginate samples. The W-450 Sonifier (Branson Schallkraft GmbH, Germany) contained a 3/499-titanium-resonator operating at a frequency of 20 kHz. For ultrasonic degradation, the concentration of alginate was adjusted to 0.1% w/w. A thermostat was used to keep the temperature of the solutions (100 mL) at 20 °C during the degradation process. The energy input (about 120 W/cm^2) induced by the resonator tip was repeatedly checked during the 4-h degradation. In order to remove metal fines abraded from the tip of the resonator, the solutions were centrifuged at 15,000*g* for 30 min and then freeze-dried.

2.6. NMR spectroscopy

For NMR spectroscopy, ultrasonically degraded, freeze-dried alginate samples were dissolved in D_2O (15 mg/mL) containing sodium-3-trimethylsilylpropionate-2,2,3,3-d_4 (TSP) as an internal reference. The ^{1}H NMR spectra were recorded using a Bruker Avance 400 NMR-spectrometer. Performance of the measurements at 70 °C sufficiently shifted the solvent peak upfield. Typically the number of scans was 128 and the spectral data were processed with a line broadening of 0.6 Hz. The solvent peak (HDO) was partly eliminated using a decoupler. Data processing (integrations and deconvolutions) was performed using the software Origin® 7.5 (OriginLab™ Corp., Northampton, USA).

2.7. Intrinsic viscosity of alginates

The specific viscosity η_{sp} of a polymer solution at very low or zero shear rate is given by Eq. 1 (known as Huggins equation; for a detailed discussion, see Kulicke and Clasen:[38]

$$\frac{\eta_{sp}}{c} = [\eta] + K_H \cdot [\eta]^2 \cdot c \quad (1)$$

where [η] is the intrinsic viscosity [mL/g] and K_H is the Huggins constant. The relationship between the intrinsic viscosity and the molar mass of the polymer at constant temperature is given by the Mark–Houwink–Sakurada (MHS) equation (Eq. 2):

$$[\eta] = K_\eta M_\eta^a \quad (2)$$

where K_η and the exponent a are empirical constants; M_η is the viscosity average molar mass.

The intrinsic viscosities of alginates were calculated from the reduced specific viscosity ($\eta_{red} = \eta_{sp}/c$). η_{red} was measured at 7–9 different concentrations within a range of the relative viscosity η_{rel} = 1.2–2.5 at 25.0 ± 0.1 °C using a Micro-Ubbelohde capillary viscometer (no. 1c; Schott-Geräte, Hofheim, Germany). Alginates were dissolved in the reference solvent.

2.8. MALS (multi-angle light scattering)

MALS is a technique allowing online and offline determination of the weight average molar mass M_w and of the coil size in terms of the z-average radius of gyration $\langle R_G \rangle_z$ of polymers in solution according to the Zimm formalism of the Rayleigh–Debye–Gans

light scattering mode.[39–43] In the offline or batch-mode, the second virial coefficient A_2 can additionally be determined. The following relation is valid:

$$\frac{K\,c}{R(\theta)} = \frac{1}{P(\theta)}\left[\frac{1}{M_w} + 2\,A_2\,c\right] \quad (3)$$

where K is the optical constant, c is the polymer (alginate) concentration, $R(\theta)$ is the Rayleigh ratio at the angle θ, and $P(\theta)$ is the particle scattering function. The optical constant is given by $K = (2\pi n_0^2/N_A\lambda^4)(dn/dc)^2$ where n is the refractive index of the solvent, λ the wavelength in vacuum (690 nm), N_A the Avogadro constant, and dn/dc is the refractive index increment of the scattering species in the solvent used. The refractive index needs to be known for the calculation of the weight average molar mass. The determination of the dn/dc values of UHV_N- and UHV_T-alginate and MALS batch measurements were carried out in the reference solvent at 25 °C. To ensure measuring at constant chemical potential the samples were dialyzed against the solvent for 12 h prior to the measurements using Spectra/Por membrane tubing (molar mass cut off: MWCO = 6–8 kDa, Spectrum Laboratories, Rancho Dominguez, USA). dn/dc values were determined using an Optilab rEX differential refractive index detector (dRI; Wyatt Technology, Santa Barbara, USA, λ = 658 nm). After dialysis sample concentration was checked colorimetrically by estimating the total carbohydrate content in 2 mL of solution using the phenol–sulfuric acid reaction.[44]

MALS batch experiments were performed by measuring the scattering intensities of different alginate concentrations at different angles using a DAWN EOS multi-angle light scattering photometer (Wyatt Technology, Santa Barbara, USA; λ_0 = 690 nm) at 25 °C. Alginate stock solutions were prepared in the same way like the solutions used for the determination of dn/dc. DAWN EOS was calibrated using suprapure toluene (Uvasol, Merck, Darmstadt, Germany) and normalized prior to every measurement using bovine serum albumin (Merck, Darmstadt, Germany). A syringe pump (Razel A-99, Razel Scientific instruments, Fairfax, USA) was used to introduce the samples into the flow cell at a constant flow rate of 0.20 mL/min.

Because of the presence of particulate substances (see below) UHV_T- and LV-alginates were centrifuged using a Beckmann Coulter ultra centrifuge (LM 8-55M, rotor TI-80). After centrifugation the concentration of the solutions was checked using the phenol–sulfuric acid reaction (see above). To remove dust the solutions were filtered prior to injection using 0.8 μm membrane filters (type AWP, Millipore, Schwalbach, Germany). Data acquisition and calculations were performed using the Astra software (v. 5.3.2; Wyatt Technology, Santa Barbara, USA).

2.8.1. SEC–MALS–dRI

For analysis of the molar mass and coil size distributions of the alginate samples size exclusion chromatography (SEC) was connected to MALS and a dRI.[45] Measurements were carried out using a solvent and sample delivery system consisting of solvent reservoir, on-line degasser, isocratic pump, and auto-injector (all units: 1100 series, Agilent Technologies, Santa Clara, USA). A size exclusion chromatography (SEC) precolumn and three analytical columns (PSS SUPREMA series: one 8 × 50 mm precolumn, particle size: 10 μm; two columns pore size: 10,000 Å, 8 × 300 mm, particle size: 10 μm; one column pore size: 100 Å, 8 × 300 mm, particle size: 10 μm; PSS Polymer Standards Service, Mainz, Germany) were serially connected.

The columns were kept at 25.0 ± 0.2 °C using a column thermostat (ECHOtherm™ CO30, Torrey Pines Scientific, San Marcos, USA). The column outlet was connected to the DAWN EOS MALS detector and to a dRI (Optilab DSP; Wyatt Technology, Santa Barbara, USA; λ_0 = 633 nm, P-100 cell). The Optilab DSP was calibrated using ultrapure NaCl (Merck, Darmstadt, Germany). Prior to the determination of the molar mass and coil size distributions M_w and $\langle R_G\rangle_z$ of the alginate samples, a pullulan standard ($M_w = 7.1 \times 10^5$ g/mol, $\langle R_G\rangle_z$ = 40 nm) was determined to verify the performance of the setup (pullulan is a well-characterized linear 1,6-linked polysaccharide used as a molar mass standard in SEC, for details see Adolphi and Kulicke[46]). To avoid shear degradation (Kulicke and Böse,[47] Bouldin et al.[34]), a flow rate of 0.5 mL/min was selected for the determination of the molar mass and coil size distribution of UHV_T- and LV-alginates. In the case of the native UHV_N-alginate sample increasing molar mass and radius of gyration were observed with increasing elution volume. This effect was reduced at lower flow rates. Measurements were carried out at a flow rate of 0.3 mL/min. The injection volume was 75–125 μl. The alginate concentration was adjusted to 0.5–1 mg/mL depending on the molar mass of the samples. Screening experiments showed that this concentration range yielded the best signal-to-noise ratio. Samples were filtered using 0.45 μm or 0.8 μm Millipore membrane filters (type AWP) prior to injection. Data from the light scattering and the differential refractometer were collected and processed using Astra software. The experimental data (slice results) were exported to an Origin® 7.5 spreadsheet for further calculations.

2.8.2. aFFFF-/MALS–dRI

The molar mass and coil size distribution of the UHV_N-alginate were also determined by asymmetrical flow-field-flow fractionation (aFFFF) coupled to MALS and dRI. This technique allows the separation of particles and macromolecules on the basis of their diffusion coefficients (for details see Kulicke et al.,[48] Roessner and Kulicke,[49] Wahlund and Giddings,[50] Schimpf et al.[51]). By contrast to SEC, aFFFF does not require a stationary phase. It has therefore fewer limitations such as sample adsorption, shear-induced degradation or exclusion limits. Measurements were carried out at 25 °C using the commercial aFFFF-System Eclipse 2 (Wyatt Technology Europe, WTE, Dernbach, Germany) on UHV_N-alginate only.

The eluent flow was provided by a solvent reservoir, an on-line degasser, isocratic pump, and auto injector (Agilent 1100 series). A short channel equipped with regenerated cellulose membrane (Millipore Ultracel MWCO 30 kDa, WTE) and a 250 μm spacer (WTE, type wide) was used (channel length: 17.3 cm; trapezoid breadths: 2.0 cm resp. 0.3 cm). Thirty microliters of the sample solution (c = 1 mg/mL) was injected into the channel. The separations were carried out using the following elution profile: prefocus 1 min, focus and inject: 2 min, postfocus 1 min; inject flow rate $\dot{V}_{inj}$ = 0.2 mL/min, focus flow rate $\dot{V}_{foc}$ = 1.5 mL/min. Elution conditions: cross-flow rate $\dot{V}_c$ = 1.1–0.07 mL/min (20 min) detector flow rate $\dot{V}_{in}$ = 2 mL/min. The outlet of eclipse 2 was connected to the DAWN EOS multi-angle light scattering photometer followed by an Optilab rEX dRI detector that was calibrated as the Optilab DSP (see above). Prior to injection samples were filtered as described under SEC–MALS–dRI, data acquisition was performed as described in the SEC–MALS–dRI section.

3. Results

3.1. Purity and dry weight of UHV-alginates

Brown algae have a high capacity to accumulate multivalent cations including very toxic heavy metals.[52] The extraction and purification process removed most metallic impurities. Data of three independent measurements are listed in Table 1. The concentrations for most heavy metals were well below 30 ppm, except for Ca and Sr, which were quite high in the UHV_N-alginate (>100 ppm). The commercial LV-alginate contained even higher concentrations of Ca than the UHV_N-alginate and also high amounts of Fe and Mg.

Table 1
Metal, chloride, and moisture contents of UHV- and LV-alginates

Element	Concentration of metal ion (mg/kg)		
	UHV_N-alginate ($n = 3$)	UHV_T-alginate ($n = 3$)	LV-alginate ($n = 2$)
Al	9.22 ± 0.30	11.92 ± 0.32	—
Ba	26.85 ± 0.55	4.32 ± 0.02	9.75 ± 0.49
Ca	155.81 ± 1.84	29.51 ± 0.18	1375 ± 45
Cd	n.d.[a]	n.d.	n.d.
Cr	2.95 ± 0.08	2.18 ± 0.15	n.d.
Cu	n.d.	n.d.	6 ± 5
Fe	16.75 ± 0.10	12.34 ± 0.10	75 ± 6
Pb	6.87 ± 0.50	n.d.	7 ± 5
Mg	28.15 ± 2.30	19.47 ± 0.90	79 ± 3
Mn	0.43 ± 0.01	0.22 ± 0.03	n.d.
Mo	n.d.	n.d.	n.d.
Ni	0.92 ± 0.16	0.75 ± 0.09	n.d.
Sn	n.d.	n.d.	n.d.
Sr	108.97 ± 3.05	0.26 ± 0.01	56.2 ± 0.2
Zn	0.94 ± 0.10	0.64 ± 0.08	—
Cl^-	1400 ± 100	5000 ± 1000	3000 ± 200
Dry weight	(84 ± 1) wt %	(86 ± 1) wt %	(85 ± 1) wt %

[a] Not detectable.

The endotoxin concentrations in purified UHV_N- and UHV_T-alginate (0.25% w/v solutions) were 7.85 ± 3.4 EU/kg and 7.86 ± 8.3 EU/kg ($n = 3$), respectively. This is much less than required for medical approval.[53] Protein impurities (Fig. 2A) were lower than those in commercial LV-alginate by factors of 80 (UHV_N) and 70 (UHV_T). Similarly, the level of immunogenic polyphenolic compounds in UHV-alginates was much lower than in commercial LV-alginates (Fig. 2B). The main reason for the absence of phenolic compounds in the UHV-alginates was the complete removal of the cell wall layer before drying and subsequent extraction. Figure 3A and B show that the cell walls of the stipes of *L. nigrescens* and *L. trabeculata* contained large amounts of insoluble phlorotannins which were mainly concentrated in the peripheral cortex cells. The amount of insoluble phlorotannins was comparable for UHV_N and UHV_T, whereas *L. nigrescens* had much less soluble phlorotannin in the cytosol than did *L. trabeculata* (Fig. 3C).

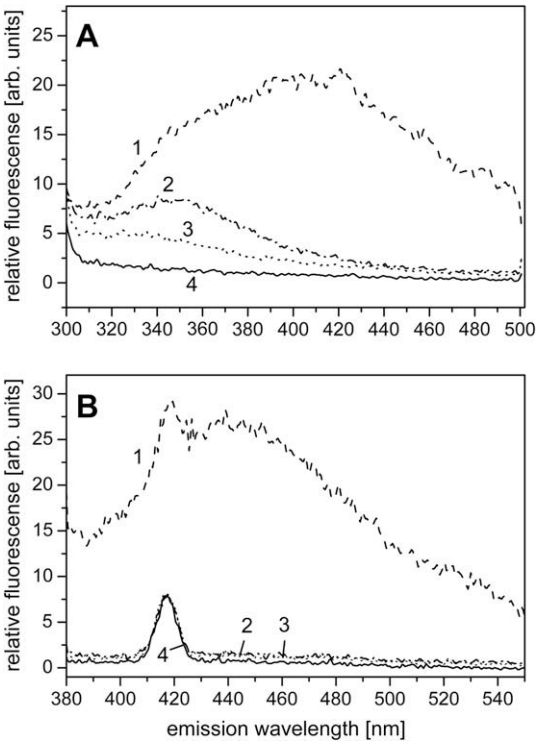

Figure 2. Fluorescence spectra of commercial low viscosity (LV) alginate (curve 1) and ultra-high viscosity (UHV) alginates extracted and purified from stipes of *Lessonia trabeculata* (UHV_T, curve 2) or *Lessonia nigrescens* (UHV_N, curve 3) after removal of the outer phlorotannine-rich cortex layer. Curve 4 represents the spectrum of distilled water. (A) Protein contaminants were determined by excitation at 270 nm and recording of the emission between 300 and 500 nm. (B) Polyphenolic-like contaminants were determined by fluorescence excitation at 366 nm; emission spectra were recorded between 380 and 550 nm. Note that UHV-alginates, but not the LV-alginate, contained practically no polyphenolic-like impurities and that also the protein content in the UHV-alginates is considerably reduced compared to LV-alginate.

For the accurate determination of viscosity and molar mass of hygroscopic polymers (such as alginates), the dry weight and the salt content of the polymer must be taken into account.[38] The chloride content of the two UHV-alginates was found to be relatively low (0.14–0.5%). Comparable values were measured for the commercial LV-alginate. Thermogravimetric measurements showed that UHV- and LV-alginates contained about 14–16% water (Table 1).

Absence of cytotoxic, mitogenic, and apoptosis-inducing ingredients in the purified alginates was demonstrated by implanting microcapsules in rodents. Microcapsules made of a 1:1 mixture of UHV_T- and UHV_N-alginate (stabilized with 0.017% poloxamer 188 and cross-linked with Ba^{2+}) were retrieved 5 weeks after implantation and showed no fibrotic or inflammatory reactions (Fig. 4). When 1% HSA was used as stabilizing additive, 1% of the retrieved microcapsules exhibited a very weak cellular overgrowth. By contrast, microcapsules made up of commercial LV-alginates evoke very strong immunological reactions (data not shown).

3.2. Chemical composition and sequence of UHV-alginates

High-resolution ^1H NMR spectroscopy on partially ultrasonically degraded UHV-alginates provided information on the guluronate to mannuronate ratios and M/G sequences. The composition and sequential structure of alginates in terms of the fractions *F* of monomers and dyad frequencies were determined according to Grasdalen et al.[54] from the peak areas. Typical ^1H NMR spectra of the anomeric region of UHV_N- and UHV_T-alginates are given in Figure 5. The peaks at 5.05 and 4.45 ppm are due to the H-1 and H-5 of the G residues in homopolymeric G blocks, respectively. The peaks that centered around 4.7 ppm arise from H-5 of MG/GM blocks and from H-1 of M residues.

Calculations of the molar fractions of F_G, F_M, and the dyad (nearest neighbor) frequencies from characteristic signals are given in Table 2. UHV_T-alginates were characterized by an extremely high G content. By contrast, UHV_N had a high M content. Both UHV-alginates also exhibited distinct differences in the heteropolymeric dyad frequencies F_{MG} and F_{GM}. Evaluation of the ^1H NMR spectra of the commercial LV-alginate (Fig. 5) yielded *F* values of intermediate monomer composition.

3.3. Intrinsic viscosity of UHV-alginates

As shown in Figure 6, the Huggins plots of the reduced viscosity versus the alginate concentration yielded linear dependencies on concentration within the measurement range of the relative viscosity ($\eta_{rel} = 1.2–2.5$). The calculated values of the intrinsic viscosity [η] of the UHV- and LV-alginates dissolved in the reference solvent at 25 °C are given in Table 3. Inspection of the table shows intrinsic viscosities up to 2750 mL/g for UHV_N-alginate. The value for UHV_T is significantly lower (1740 mL/g), but still much higher than that of commercial LV-alginate (970 mL/g). Determination of the intrinsic viscosities at different salt concentrations showed that the polyelectrolyte effect is sufficiently suppressed at the concentration of the reference solvent, which is in agreement with the

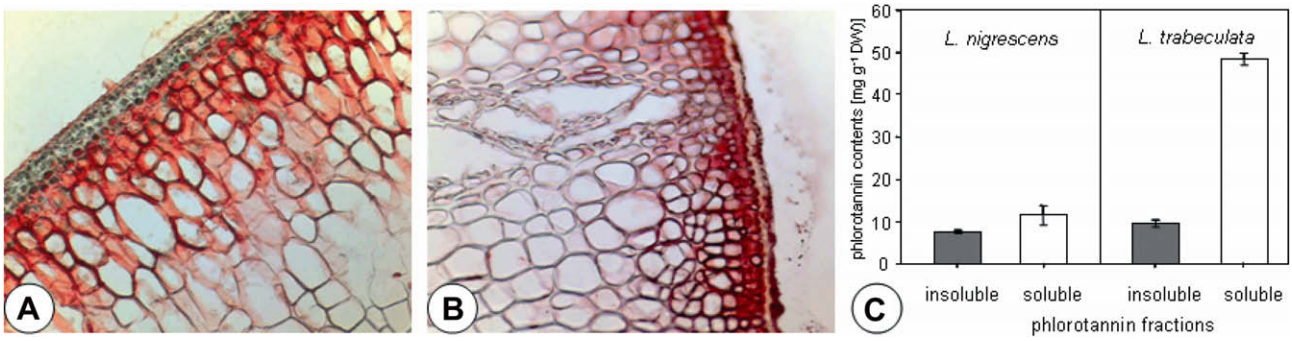

Figure 3. Distribution of phlorotannins (stained with vanillin-HCl) in the cross-sections of the stipes of *L. nigrescens* (A) and *L. trabeculata* (B). The histograms in (C) gave the amount of phlorotannin (mg/g dry weight) in the cell walls (outer cortex; insoluble fraction) and in the cytosol (soluble fraction) of the two species.

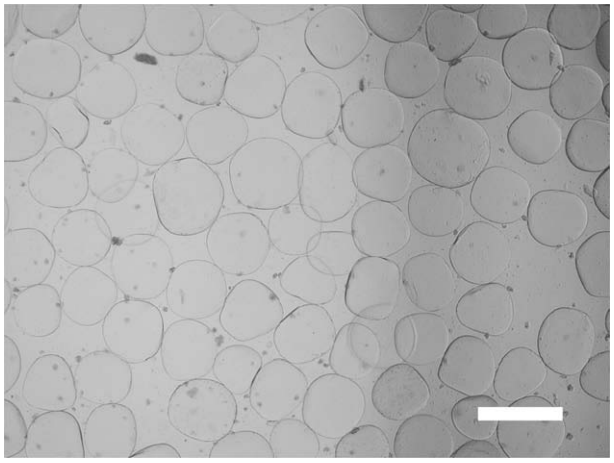

Figure 4. Ba^{2+} cross-linked UHV-alginate microcapsules retrieved after 5 weeks of implantation in the peritoneum of Balb/c mice. Note that microcapsules made up of a 1:1 mixture of UHV_T- and UHV_N-alginates (so-called UHV_{NT}-alginates) did not provoke any fibrotic overgrowth. Microcapsule formation was made by using an air-jet droplet generator with a nozzle diameter of 500 μm. Internal gelling was performed by bombardment with $BaCl_2$ crystals (for details see, Zimmermann et al.[31]). Bar = 400 μm.

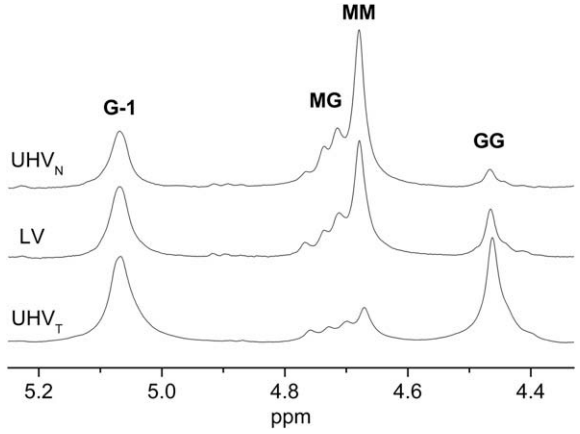

Figure 5. Anomeric region in the 400 MHz ^1H NMR spectra of UHV_N-, UHV_T-, and LV-alginates. The spectra were recorded after partial ultrasound degradation in order to achieve high-resolution spectra. Calculations of the fractions, *F*, of M and G monomers and monomer sequences from the spectra were performed according to Grasdalen et al.[54] UHV_T-alginate was characterized by an extremely high G-content ($F_G = 0.78$; $F_{GG} = 0.67$) and UHV_N by a fairly high M-content ($F_M = 0.61$; $F_{MM} = 0.29$). The corresponding values of LV-alginate were calculated to be $F_G = 0.58$, $F_{GG} = 0.23$, $F_M = 0.42$, $F_{MM} = 0.06$, and $F_{GM} = F_{MG} = 0.35$.

findings of Smidsrød and Haug.[55] The very high values of the intrinsic viscosity indicate high molar masses of UHV-alginates that could be experimentally proved.

3.4. Average molar mass and coil size of UHV-alginates

The weight average molar mass, M_w, the *z*-average radius of gyration, $\langle R_G \rangle_z$, and the second virial coefficient, A_2, of the alginates were determined using MALS in the batch mode. Calculation of these parameters requires knowledge of the refractive index increment, d*n*/d*c*. d*n*/d*c* values of UHV_N- and UHV_T-alginates showed that the refractive index, *n*, depended linearly on the concentration, *c* (from 1×10^{-5} to 1×10^{-3} g/mL; data not shown). The experiments yielded 0.153 mL/g for UHV_N and 0.151 mL/g for UHV_T. The values are very close to the d*n*/d*c* values previously reported for alginates.[56,57] For calculations of the molar mass of the LV-alginate, we used an average value of 0.152 mL/g.

By contrast to UHV_N-alginate, MALS measurements on filtered UHV_T- and on LV-alginate samples led to non-reproducible results and unreasonable low or even negative values of the second virial coefficient A_2. This was obviously due to the very noisy signals (signal-to-noise ratio close to unity). This phenomenon is often observed if alginates or other polymers contain particulate material.[55,56,58–63] Extended ultracentrifugation of UHV_T- and LV-alginates at >100,000*g* considerably reduced the content of the particulate components.[55,56,59] However, ultracentrifugation also reduced the concentration of UHV-alginates. Variation of the centrifugation rates over a large range together with simultaneous determinations of the second virial coefficient showed that centrifugation at 40,000*g* for 2.5 h yielded the best results. Under these conditions a concentration reduction of 4% for UHV_T- and of 6% for LV-alginate occurred, reflecting the amount of particulate components (data not shown).

Table 2
Sequential structure of alginates

Alginate	F_M	F_G	M/G	F_{MM}	F_{MG}	F_{GM}	F_{GG}
UHV_T	0.22	0.78	0.28	0.10	0.11	0.11	0.67
UHV_N	0.61	0.39	1.55	0.29	0.32	0.32	0.08
LV	0.42	0.58	0.71	0.06	0.35	0.35	0.23

Fractions *F* and ratio of manuronic and guluronic acid and block structure of UHV_N-, UHV_T-, and LV-alginates determined by ^1H NMR spectroscopy.

The Zimm plots of UHV_N-, UHV_T-, and LV-alginates showed the typical appearance. As an example the Zimm plot of UHV_N-alginate is depicted in Figure 7. The angular dependency of the scattered light intensities was fitted by a second order fit, whereas the concentration dependency was fitted by using the least square

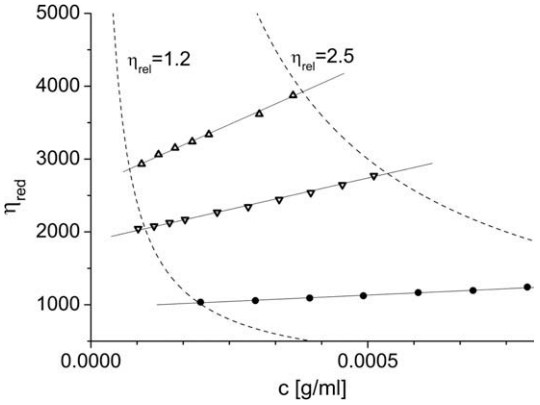

Figure 6. Huggins-Plot of the reduced viscosity, η_{red}, as a function of the concentration, c, of the UHV_N- (Δ), UHV_T- (∇), and of LV-alginates (O) dissolved in reference solvent. Fits were made by the least squares method.

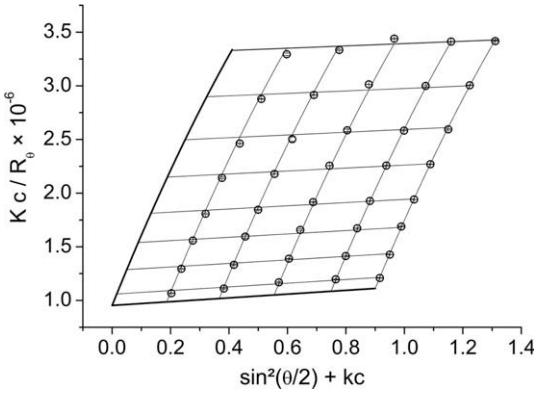

Figure 7. Typical Zimm-Plot (i.e., angular- and concentration dependence of the scattered light intensities) of UHV_N-alginate dissolved in reference solvent. Calculations yielded $M_w = 1.1 \times 10^6$ g/mol, $\langle R_G \rangle_z = 191$ nm, and $A_2 = 3.7 \times 10^{-3}$ mol mL/g^2.

method. The values of M_w, $\langle R_G \rangle_z$, and A_2 of the UHV- and LV-alginates calculated from the plots by using Eq. 3 are given in Table 3. The average M_w of the UHV-alginates was 2–4 times that of the commercial LV-alginate. Equally, the coil size expressed by the z-average radius of gyration was also significantly larger for UHV-alginates than that of the commercial LV-alginate.

The A_2 value of the UHV_N-alginate was slightly higher compared to that of UHV_T-alginate, while the A_2 value of the LV-alginate remained slightly negative indicating that the particulate substances were not completely removed by centrifugation. Measurements on UHV_T immediately and 48 h after centrifugation yielded similar results, suggesting a particulate impurity in the starting material rather than a reversible aggregation of the macromolecules (see Section 4).

3.5. Determination of the molar mass and coil size distribution of UHV-alginates

The distribution of the molar mass and the coil size of the alginate samples was determined by using SEC coupled online to MALS and dRI. Triplicate experiments were carried out for each sample. The recovery rate of the fractionated samples, (i.e., the fraction of polymer that reached the differential refractometer) was in the range of 83–96%. Typical chromatograms of the UHV- and LV-alginates are depicted in Figure 8A. Under equilibrium and ideal SEC conditions the elution volume should be independent from the molar mass and coil size of a substance and the corresponding progressions over the elution volume should overlap. However Figure 8A shows a different elution behavior indicating non-ideal, incomplete separation of UHV alginates (see Section 4). It is obvious from the broad mass distribution of the LV-alginate that LV appears more disperse than are the UHV-alginates. Interestingly, the chromatogram of the UHV_T-alginate exhibits a slight shoulder at low molar mass, presumably due to the presence of dense particulate substances.

From the elution curves the average value of the molar masses of the UHV-alginates is a factor of 2–4 higher than that of the commercial LV-alginate. Similarly, UHV-alginates exhibit significantly higher values of the radius of gyration than the commercial LV-alginate (see Table 3). The M_w and $\langle R_G \rangle_z$ values were by about 10% smaller than those determined by MALS in the batch mode. This finding is presumably due to the exclusion of aggregates and/or larger microgel particles that are filtered out by the columns (see Section 2). Furthermore, inspection of the chromatograms of the UHV-alginates shows an increase in M_w and particularly in $\langle R_G \rangle_z$ with increasing elution volume.

Typical cumulative molar mass and coil size distributions of UHV- and commercial LV-alginates confirmed the above results. It is evident from Figure 8B that the UHV_N-alginate consists of high molar mass fractions ranging from 3.3×10^5 to 2.9×10^6 g/mol and exhibits high radii of gyration ranging from 98 nm to 300 nm. Similarly, the UHV_T-alginate contains molar mass frac-

Table 3
Physicochemical properties of alginates obtained by SEC–MALS–dRI, aFFFF–MALS–dRI, MALS-batch, dRI-batch, and capillary viscometry

Sample	SEC–MALS–dRI		aFFFF–MALS–dRI		MALS-batch			dRI	CV
	$M_n/M_w \times 10^{-5}$ (g/mol)	$\langle R_G \rangle_z$ (nm)	$M_n/M_w \times 10^{-5}$ (g/mol)	$\langle R_G \rangle_z$ (nm)	$M_w \times 10^{-5}$ (g/mol)	$\langle R_G \rangle_z$ (nm)	$A_2 \times 10^3$ (mol mL/g^2)	dn/dc (mL/g)	$[\eta]$ (mL/g)
UHV_N, native	7.1/9.7	173	8.3 / 10.0	173	10.7 ± 0.1	191 ± 2	3.7	0.153	2750
UHV_N, 1 min	4.9/7.3	164							2200
UHV_N, 3 min	4.2/6.9	154							2080
UHV_N, 6 min	3.4/5.8	143							1850
UHV_N, 12 min	2.3/4.0	116							1390
UHV_N, 15 min	2.1/3.5	108							1240
UHV_T, native	3.7/5.5	136			5.6 ± 0.1	140 ± 5	3.4	0.151	1740
UHV_T, 3 min	2.8/4.6	126							1570
UHV_T, 6 min	2.7/4.1	111							1460
UHV_T, 9 min	2.5/3.5	100							1200
UHV_T, 12 min	2.1/3.0	88							1100
UHV_T, 15 min	1.6/2.3	77							920
LV, native	1.4/2.3	80			2.9 ± 0.1	108 ± 2	−4.0		970

CV: capillary viscometry (micro-ubbelohde).

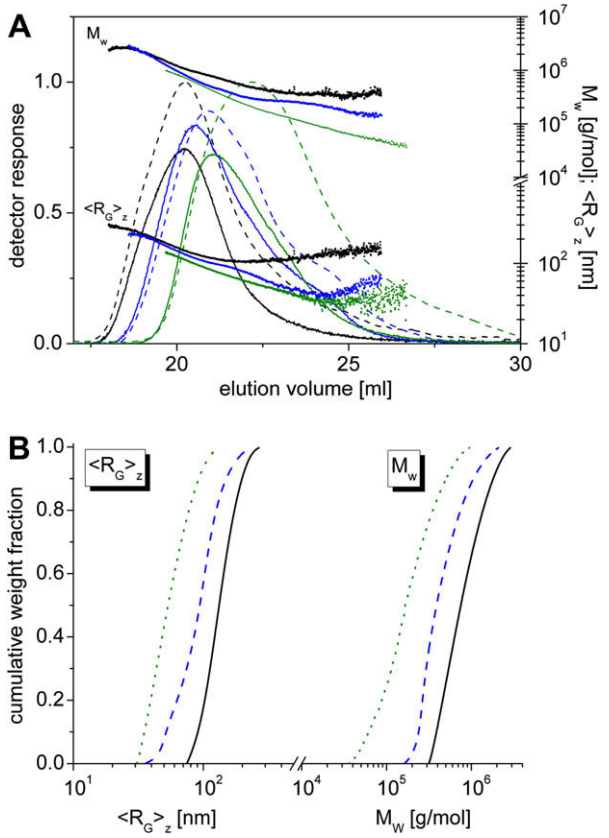

Figure 8. Typical chromatograms (A) and the absolute cumulative distributions of the radius of gyration and the molar mass (B) of LV- and UHV-alginates determined by SEC–MALS–dRI. (A) MALS response at 90°: solid lines, dRI response: dashed lines; LV-alginate: green lines, UHV_T: blue lines and UHV_N: black lines. The calculated values of M_w and $\langle R_G\rangle_z$ of the LV- and UHV-alginates are colored accordingly. (B) LV (dotted line), UHV_T (dashed line), and UHV_N (solid line). Note that SEC–MALS–dRI yielded comparable average values for M_w and $\langle R_G\rangle_z$ for UHV-alginates as MALS (see Fig. 7 and Table 3), whereas the corresponding values of the LV-alginate were considerably smaller.

tions ranging from 1.4×10^5 to 2.6×10^6 g/mol and radii of gyration from 40 nm to 230 nm. By contrast, the molar mass and the radii of gyration of the commercial LV-alginate are much smaller. Molar mass ranges from 3.6×10^4 to 9.0×10^5 g/mol and the corresponding radii of gyration range from ~25 nm (detection limit; $\langle R_G\rangle$ approaches $\lambda/20$) to 130 nm. Additionally the portion of lower molar mass/radius of gyration macromolecules observed in case of the LV-alginate is significantly smaller than that measured for UHV-alginates, especially for the UHV_N-alginate reflecting a negligible degradation of alginate chains during the collection and extraction process of UHV-alginates.

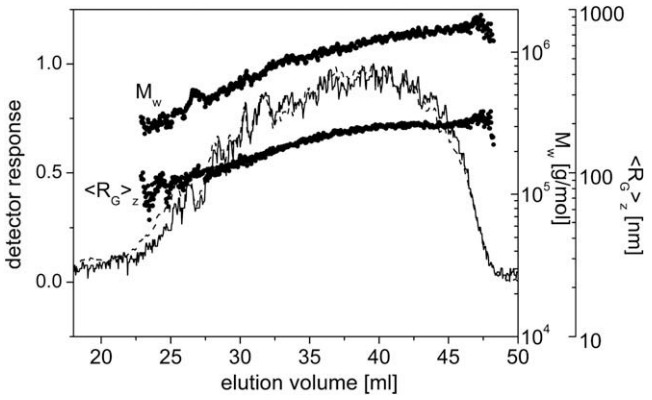

Figure 9. A typical chromatogram of UHV_N-alginate determined by aFFFF–MALS–dRI. MALS response at 90°: solid lines, dRI response: dashed lines. The average M_w and $\langle R_G\rangle_z$ values agreed quite well with the corresponding values derived from MALS (Fig. 7) and SEC–MALS–dRI (Fig. 8); see also Table 3.

To investigate possible effects of the fractionation technique on the determination of the M_w and $\langle R_G\rangle_z$ of UHV-alginates, the highest molar mass alginate UHV_N was also analyzed using asymmetrical flow-field-flow fractionation (aFFFF) coupled to MALS and dRI. A typical aFFFF chromatogram of UHV_N-alginate is depicted in Figure 9. The average values of M_w and $\langle R_G\rangle_z$ were 1×10^6 g/mol and 173 nm, that is, in the order of magnitude calculated from MALS batch and SEC–MALS–dRI measurements, the recovery rate was 96%. Inspection of the curves shows that the polydispersity index (PDI, i.e., the ratio M_w/M_n) is reduced from 1.4 to 1.2. However, in contrast to the results obtained by SEC–MALS–dRI no abnormal elution behavior regarding M_w and $\langle R_G\rangle_z$ was detected, indicating that this phenomenon is an artifact caused by SEC fractionation.

3.6. Dependence of the radius of gyration and the intrinsic viscosity on molar mass

Alginate fractions of intermediate molar mass, different radii of gyration, and different intrinsic viscosity were prepared by partial ultrasonic degradation of the UHV-alginates. The weight average molar mass and the *z*-average radius of gyration of the samples were determined by means of SEC–MALS–dRI and are listed in Table 3.

The conformation plot (plot of the logarithm of the weight average molar mass against the radius gyration) of ultrasonic degraded

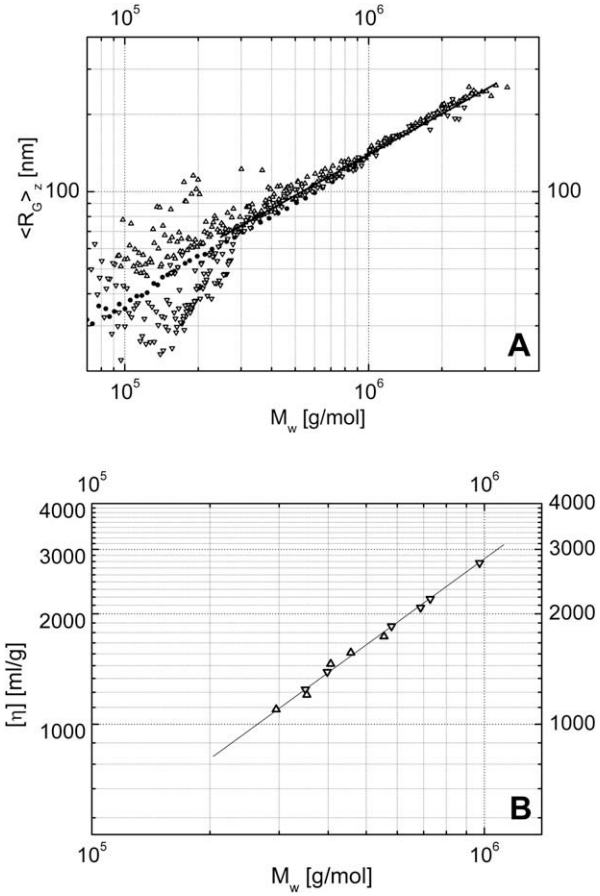

Figure 10. Plot of log $\langle R_G\rangle_z$ versus log M_w (so-called conformation plot; A) and of the logarithm of the intrinsic viscosity [η] versus log M_w (so-called Mark–Houwink–Sakurada plot; B) of low, intermediate, and ultra-high viscosity alginates (LV (O) in A; UHV_N (Δ), UHV_T (∇) in A and B). Alginates were dissolved in the reference solvent.

and native UHV_N- and UHV_T-alginate fractions and LV-alginate is depicted in Figure 10a (for clarity only part of the data are given). Due to the scattering of the data at low molar mass, a $\langle R_G \rangle$–M-relationship could only be established for the linear regions of curves. The analysis yielded the following $\langle R_G \rangle$–M-relationship for the UHV- and LV-alginates:

$$\begin{aligned} &UHV_N: \quad \langle R_G \rangle_z = 0.103 \times M_w^{0.52\pm0.02} \ (5.0 < M_w < 27.0) \times 10^5 \text{ g/mol} \\ &UHV_T: \quad \langle R_G \rangle_z = 0.093 \times M_w^{0.53\pm0.01} \ (3.0 < M_w < 26.0) \times 10^5 \text{ g/mol} \\ &LV: \quad \langle R_G \rangle_z = 0.073 \times M_w^{0.54\pm0.01} \ (0.5 < M_w < 09.0) \times 10^5 \text{ g/mol} \end{aligned} \tag{4}$$

It is obvious that the exponent ν of the low and ultra-high viscosity alginates was nearly identical.

The intrinsic viscosity data measured on native and ultrasonically degraded UHV-alginates could be fitted in the M_w range between 3×10^5 and 1×10^6 g/mol:

$$[\eta] = 0.059 \times M_w^{0.78\pm0.02} \tag{5}$$

Consistent with this, a double logarithmic plot of the intrinsic viscosity versus the weight average molar mass of the alginate fractions (a so-called Mark–Houwink–Sakurada plot) of UHV-alginate yielded a straight line (Fig. 10b).

4. Discussion

Composition, structure, and purity of biopolymers depend strongly on the origin and quality of the raw material and on the subsequent extraction process. Alginates are very good examples. UHV-alginates extracted from stipes of brown algae which are harvested freshly from the sea, peeled, treated with antimicrobial agents, and subjected to O_2-plasma treatment before subjection to a tailored extraction process differ considerably in purity, molar mass, and other relevant physico-chemical properties from commercial LV-alginates. Commercial alginates are usually extracted from the stipes and blades of brown algae washed ashore by the tide and by the wind. The dried material is highly polluted and degradation processes start long before the material is collected. As shown in Table 1, UHV-alginates extracted from *L. nigrescens* and *L. trabeculata* have low content of (heavy) metal ions. Calcium in the final product is also much lower than in commercial alginates. Contamination with protein is negligible. Insoluble (cytotoxic) phlorotannins located in the outer cell walls (Fig. 3) are removed by peeling the stipes. The extraction process removes soluble phlorotannins and other phenolic substances (see Fig. 2). The absence of other immunogenic substances such as lipopolysaccharides, phospholipids, chlorophyll, and toxins (brown algae are frequently overgrown with epiphytes) is demonstrated by the lack of any significant immunological response upon implantation of Ba^{2+} cross-linked UHV-alginates into rodents (Fig. 4; see also Zimmermann et al.[64] and Leinfelder et al.[27]).

The quality, composition, structure, viscosity, and molar mass distribution must be known and guaranteed if alginates are to be routinely implanted into humans. Composition and sequential structure of UHV-alginates were determined using NMR spectroscopy (Fig. 5).[52,54,65] Measurements were performed on ultrasonically degraded alginate samples in order to increase the signal-to-noise ratio,[35,66] because high viscosities lead to an increase in the relaxation times and therefore to a reduced resolution. The molar fractions of F_M and F_{MM} calculated from the spectra (see above and Grasdalen et al.[54]) were quite high for UHV_N-alginate and were very low for UHV_T-alginate. Both UHV-alginates also showed distinct differences in the heteropolymeric dyads. The high $F_G = 0.78$ and $F_{GG} = 0.67$ values measured here for UHV_T-alginates were significantly smaller than the values reported by Venegas et al.[67] Reasons for this discrepancy between our finding and the literature may include modifications in alginate biosynthesis due to variable environmental conditions. Some support for this assumption was reported by Indergaard et al.[68] and Venegas et al.[67]

Gel stiffness increases in the order: MG-blocks < MM-blocks < GG-blocks and elasticity in the order: GG-blocks < MM-blocks < MG-blocks.[16] This explains why a 1:1 mixture of UHV_N- and UHV_T-alginates gives gels that are both mechanically stable and highly elastic. Termed UHV_{NT}-alginate, this mixture has been used successfully in immunoisolated transplantation and to form alginate membranes, see Figure 4.[4,11,12] The F_G value of UHV_{NT}-alginate is comparable to the value measured here for the commercial LV-alginate. However, there is a wealth of experimental evidence (see Zimmermann et al.[4,10,12]) that commercial LV-alginate yields microcapsules of lower long-term stability and elasticity than UHV_{NT}-alginates. These differences may stem from differences in the intrinsic viscosity.

As shown here UHV-alginates dissolved in 0.154 mol/mL sodium chloride exhibit an extremely high intrinsic viscosity $[\eta]$ (see Fig. 6 and Table 3). The intrinsic viscosity of UHV_{NT}-alginates is much higher than $[\eta]$ for LV-alginate. These findings justify, retrospectively, the name *ultra-high viscosity* for this class of alginates since alginates of much lower viscosity were termed *high viscosity* alginates in the literature.[12] The lower $[\eta]$ value of UHV_T-alginate compared to that of UHV_N-alginate is probably due to the treatment of the algae before extraction with cold HCl which led to some depolymerization of the polymeric chains. HCl pre-treatment of the stipes is necessary because of the tight binding of the alginate in *L. trabeculata*. The HCl pre-treatment seems also to be responsible for the somewhat higher concentrations of chloride in the final purified product (see Table 1).

The high $[\eta]$ values of UHV-alginates suggest a high molar mass of this class of alginates. This could be confirmed by absolute determination of the molar mass and coil size of UHV-alginates by means of MALS in the batch mode and coupled techniques such as SEC–MALS–dRI and aFFFF–MALS–dRI that give absolute molar mass distribution and coil size distribution. An advantage of MALS in the batch mode over the two other fractionation procedures is that this technique yields mean values of the molar mass M_w, the radius of gyration $\langle R_G \rangle_z$, and of the second virial coefficient without any substance loss. As mentioned above, particulate substances interfere with MALS measurements and are manifested by negative values of A_2.[55,56,58–63] They were present in UHV_T-alginates and particularly in the LV-alginate, but could surprisingly not be detected in the UHV_N-alginate (see Table 3; Figs. 8 and 9). The concentration of the particulate substances could be reduced and somewhat quantified by ultracentrifugation and simultaneous detection of the change in alginate concentration as well as of the second virial coefficient at the expense of a small loss of alginate. Even though the measurement of A_2 was a good indicator for the removal of particular substance, the accuracy of the values was limited. However, the A_2 value of $3.2–3.7 \times 10^{-3}$ mol mL/g^2 determined for the two UHV-alginates was in reasonable agreement with the values determined by Smidsrød and Haug,[55] and Mackie et al.[56] at an ionic strength of $I = 0.1$. On the other hand, our A_2 value was significantly lower than the value determined by Vold et al.[59] Since the accuracy of the determination of A_2 was obviously limited, the dependence of A_2 on the molar mass was not further investigated.

From the Zimm plots of the MALS batch data (Fig. 7) a weight average molar mass of $M_w = 1.1 \times 10^6$ g/mol for UHV_N- and 5.6×10^5 g/mol for UHV_T-alginates was calculated. The corresponding average values for the radius of gyration were $\langle R_G \rangle_z = 191$ nm (UHV_N) and $\langle R_G \rangle_z = 136$ nm (UHV_T). Independent determination of M_w and $\langle R_G \rangle_z$ using SEC–MALS–dRI (Fig. 8) and aFFFF–MALS–dRI (Fig. 9) yielded average values of M_w and $\langle R_G \rangle_z$ values that agreed well with those obtained by the batch measure-

ments. The slightly smaller values are most likely caused by incomplete sample recovery (see Table 3). The distributions of the molar mass and of the radii of gyration (see Fig. 8) also support the conclusion that UHV-alginates, especially UHV_N, exhibit higher molar mass fractions than LV-alginate.

The values of the number average molar mass M_n calculated from the slice results of the chromatogram shown in Figure 8 assuming monodisperse fractions are comparatively large. These values are most likely overestimated because of the already mentioned incomplete separation by SEC that becomes manifested in increasing values of M_w and especially of $\langle R_G\rangle_z$ with proceeding elution (Fig. 8). Obviously, the separation of UHV alginate components in the columns is not the result of a simple equilibrium between exclusion and permeation of the macromolecules in the stationary phase, but of complex processes, summarized by Giddings[60] and reported for ultra-high molar mass polyethylene oxide by Porsch et al.[61] These include flow suppression in pores, shear degradation, polarization effect, hydrodynamically induced diffusion, stress-induced diffusion, and multipath effect and lead to retardation of large coils, while hydrodynamic chromatography mode leads to accelerated elution. Also nonlinear effects such as viscous fingering, recently summarized by Rousseaux et al.[62] have to be considered for the separation of ultra-high viscosity/molar mass polymers using SEC.

In the present study the effects were significantly reduced by optimization of the sample concentration and the flow rate, further reduction should be achieved using columns with bigger particle sizes. The additional delay that UHV sample fractions are exposed result in coelution with LV fractions and leads to elution volumes with inhomogeneous molar mass. Such a behavior is only detectable with a molar mass and/or size-sensitive detector such as an MALS detector. In the presence of polydisperse fractions MALS provides M_w and $\langle R_G\rangle_z$ average values. A direct result is the over-estimation of the calculated M_n value, leading to apparently narrow distributions. Fortunately, like theoretically expected, global mean values of M_w and $\langle R_G\rangle_z$ were not affected (see Table 3).

Vold et al.[59] found a similar elution behavior for LV-alginates extracted from *Laminaria hyperborea*. These authors ascribed this phenomenon to the presence of particulate substances. However, this explanation may be questionable because the unusual elution behavior was less pronounced (or even absent) with LV-alginates and they contained the largest amount of particulate compounds. Rather, the results obtained by aFFFF–MALS–dRI for the UHV_N-alginate suggest that the elution behavior is based on the described artifacts arising from SEC-fractionation.

Inspection of Figures 8 and 9 shows that the distribution of the two parameters is narrow compared to LV-alginate. The PDI value calculated from SEC–MALS–dRI measurements is 1.4 for UHV_N-alginate and 1.5 for UHV_T-alginate (Table 3). For LV-alginate a value of 1.6 is calculated. The low PDI values of the UHV-alginates most likely arise from the described SEC artifacts that reduce the resolution, particularly in the lower regions of the distributions. Unfortunately, the low resolution impedes the investigation of the influence of parameters like extraction conditions or season of harvest on these parameters. Nevertheless, inspection of the dRI-signals of LV-alginates in Figure 8 clearly shows higher amounts of low molar mass fractions at elution volumes >25 mL than for UHV-alginates.

aFFFF–MALS–dRI measurements yielded an even smaller PDI of 1.2 for UHV_N (Table 3). However, the absence of a comparable, unusual elution behavior like in SEC-fractionation indicates its origin in SEC-fractionation to be the non-ideal fractionation mechanism for UHV alginates. SEC was favored for separations because the variation of the separation conditions in aFFFF (channel length, spacer size, and force-field-program) led to higher PDI values, but diminished accuracy because of poor dRI baseline stability (data not shown).

The plot of log $\langle R_G\rangle_z$ versus log M_w (so-called conformation plot; Eq. 4) for the LV-alginate based on data obtained from SEC–MALS–dRI (Fig. 10) yielded a straight line as also reported by Vold et al.[59] for LV-alginates. By contrast, UHV-alginates exhibited a large scatter of the $\langle R_G\rangle_z$ data in the low molar mass region that was most likely caused by fractionation artifacts. Toward larger molar mass, the data could be fitted by a straight line over a large molar mass range. The value of the slope of these straight lines (Eq. 4) of the $\langle R_G\rangle_z$–M_w-dependency is practically identical for the two UHV-alginates ($\nu = 0.52$ and 0.53, respectively). This suggests that the monomer composition has no influence on the coil expansion. Vold et al.[59] came to the same conclusion whereas Mackie et al.[56] found an effect of the monomer composition on coil expansion. The ν value of the LV-alginate was only slightly, if at all, higher than that of the UHV-alginates and agrees quite well with the value reported by Smidsrød and Haug.[55] The authors measured the $\langle R_G\rangle_z$–M_w-dependency for intermediate and high molar mass alginates at an ionic strength of I = 0.1. Extrapolation of the linear part of the $\langle R_G\rangle_z$–M_w-relationship of Smidsrød and Haug[55] to the molar mass of 1.1×10^6 g/mol predicts an average value of $\langle R_G\rangle = 174$ nm for the UHV-alginates. This value is very close to the value determined here. Thus, we can conclude that UHV-alginates exhibit a random coil structure similar to that of LV-alginates.

A slightly expanded solution structure is suggested by the $\log[\eta] - \log M_w$ dependency (see Fig 10.). By contrast to the $\log\langle R_G\rangle_z - \log M_w$-relation, data are not scattered in the low molar mass range. Furthermore, the data sets of both UHV_N and UHV_T could be fitted by a single equation (Eq. 4) indicating that the monomer composition has obviously no significant effect on coil expansion within the range of molar mass investigated here. The exponent a in Eq. 5 is—like ν—a measure for coil expansion and is calculated to be 0.78 at $I = 0.154$.

The value is between those calculated by Smidsrød and Haug,[55] ($a = 1.0$), Mackie et al.[56] ($a = 1.00$–1.11), and Vold et al. ($a = 0.66$)[69] for alginates of intermediate and high molar mass at $I = 0.1$. It is still high enough to conclude an expanded solution structure. The variance of the parameter a in the literature demonstrates, that determination of the molar mass (generally by classical light scattering) and of the intrinsic viscosity (generally by capillary viscometry) of alginates is not trivial. As a consequence, the calculated viscosity average molar mass of an alginate sample differs significantly, depending on the set of data used. Most likely this is caused by varying amounts of particulate impurities that are most often present in alginates and by different sample preparation methods used to minimize their influence. These differences are not a solid basis for comparison of the solution structure of LV and UHV alginates and/or of alginates from different origins. A comparison with literature data is therefore questionable. Unlike the $\langle R_G\rangle_z$ data obtained for the commercial LV alginate and UHV alginates, not enough [η]-data points were obtained for a comparison of the conformation of LV and UHV alginates in solution.

In the light of the Fox–Flory-equation[70] an a value of 0.78 would predict a ν value of 0.59. The reason for this discrepancy may be that the Flory's θ-concept represents an oversimplification when applied to highly charged UHV-alginates. The theory does not consider the specific interactions between solvent and polymers that cannot be ignored in highly polar solutions.

To sum up, we have demonstrated with a broad array of techniques that UHV-alginates extracted from fresh stipes of *L. nigrescens* and *L. trabeculata* are nearly free of impurities and have a very high molar mass compared to previously reported LV alginates. These two features are most probably responsible for the finding by Zimmermann et al.[2] that the demixing of polymeric chains observed with LV-alginates is not seen during cross-linking of UHV

alginate mixtures with divalent cations. This is important as homogeneously cross-linked microcapsules exhibit long-term mechanical stability and elasticity.[2,4,12,19,71] The $\langle R_G\rangle_z$–M_w- and $[\eta]$–M_w-relationships derived from MALS and capillary viscometry measurements were practically identical for UHV_N- and UHV_T-alginates, indicating that the monomer composition has no effect on the solution structure. Thus, capillary viscometry is a simple method for validation of the extraction and purification process of UHV-alginates. Changes in molar mass (depolymerization processes) can practically be monitored in real time. Furthermore, molar mass and coil size of mixtures of UHV-alginates (as used successfully for the manufacturing of immuno-isolated microcapsules; see above) can easily be determined by viscometry measurements.

Acknowledgments

This work was supported by grants from the Bundesministerium für Bildung und Forschung (BMBF) to U.Z. and H.Z (μAirjet 0313680B), and by grants from the University Hamburg to W.-M.K. and from the Conicyt Chile (Fondecyt 1060503) to I.G.

References

1. Hasse, C.; Klöck, G.; Schlosser, A.; Zimmermann, U.; Rothmund, M. *Lancet* **1997**, *350*, 1296–1297.
2. Zimmermann, U.; Mimietz, S.; Zimmermann, H.; Hillgärtner, M.; Schneider, H.; Ludwig, J.; Hasse, C.; Haase, A.; Rothmund, M.; Fuhr, G. *Biotechniques* **2000**, *29*, 564–581.
3. de Vos, P.; Faas, M. M.; Strand, B.; Calafiore, R. *Biomaterials* **2006**, *27*, 5603–5617.
4. Zimmermann, H.; Shirley, S. G.; Zimmermann, U. *Curr. Diab. Rep.* **2007**, *7*, 31–320.
5. Kühtreiber, W. M.; Lanza, R. P.; Chick, W. L. *Cell Encapsulation Technology and Therapeutics*; Birkhäuser: Boston, 1999.
6. Lanza, R. P.; Langer, R.; Vacanti, J. *Principles of Tissue Engineering;*; Academic Press: San Diego, 2000.
7. Hoffman, A. S. *Adv. Drug Delivery Rev.* **2002**, *54*, 3–12.
8. Tønnesen, H. H.; Karlsen, J. *Drug Dev. Ind. Pharm.* **2002**, *28*, 621–630.
9. Weber, M.; Steinert, A.; Jork, A.; Dimmler, A.; Thürmer, F.; Schütze, N.; Hendrich, C.; Zimmermann, U. *Biomaterials* **2002**, *23*, 2003–2013.
10. Zimmermann, H.; Zimmermann, D.; Reuss, R.; Feilen, P. J.; Manz, B.; Katsen, A.; Weber, M.; Ihmig, F. R.; Ehrhart, F.; Geßner, P.; Behringer, M.; Steinbach, A.; Wegner, L. H.; Sukhorukov, V. L.; Vásquez, J. A.; Schneider, S.; Weber, M. M.; Volkes, F.; Wolf, R.; Zimmermann, U. *J. Mater. Sci. Mater. Med.* **2005**, *16*, 491–501.
11. Zimmermann, H.; Wählisch, F.; Baier, C.; Westhoff, M.; Reuss, R.; Zimmermann, D.; Behringer, M.; Ehrhart, F.; Katsen-Globa, A.; Giese, C.; Marx, U.; Sukhorukov, V. L.; Vásquez, J. A.; Jakob, P.; Shirley, S. G.; Zimmermann, U. *Biomaterials* **2007**, *28*, 1327–1345.
12. Zimmermann, H.; Ehrhart, F.; Zimmermann, D.; Müller, K.; Katsen-Globa, A.; Behringer, M.; Feilen, P. J.; Geßner, P.; Zimmermann, G.; Shirley, S. G.; Weber, M. M.; Metze, J.; Zimmermann, U. *Appl. Phys. A* **2007**, *89*, 909–922.
13. Vermeulen, H.; Ubbink, D. T.; Goossens, A.; de Vos, R.; Legemate, D. A. *Br. J. Surg.* **2005**, *92*, 665–672.
14. Liew, C. V.; Chan, L. W.; Ching, A. L.; Heng, P. W. S. *Int. J. Pharm.* **2006**, *309*, 25–37.
15. Rees, D. A.; Welsh, E. J. *Angew. Chem., Int. Ed.* **1977**, *16*, 214–223.
16. Draget, K. I.; Gaserød, O.; Aune, I.; Andersen, P. O.; Storbakken, B.; Stokke, B. T.; Smidsrød, O. *Food Hydrocolloids* **2001**, *15*, 485–490.
17. Donati, I.; Holtan, S.; Morch, Y. A.; Borgogna, M.; Dentini, M.; Skjåk-Bræk, G. *Biomacromolecules* **2005**, *6*, 1031–1040.
18. Mattiasson, B. Immobilization Methods. In *Immobilized Cells and Organelles*; Mattiasson, B., Ed.; CRC Press: Boca Raton, FL, 1982; Vol. I, pp 3–26.
19. Schneider, S.; Feilen, P. J.; Brunnenmeier, F.; Minnemann, T.; Zimmermann, H.; Zimmermann, U.; Weber, M. M. *Diabetes* **2005**, *54*, 687–693.
20. Edding, M.; Fonck, E.; Orrego, P.; Venegas, M.; Macchiavello, J. *Hydrobiologia* **1993**, *260/261*, 231–237.
21. Martínez, E. A. *Hydrobiologia* **1996**, *326/327*, 205–211.
22. Martínez, E. A. *Pac. Sci.* **1999**, *53*, 74–81.
23. Martínez, E. A.; Cárdenas, L.; Pinto, R. *J. Phycol.* **2003**, *39*, 504–508.
24. Tala, F.; Edding, M.; Vásquez, J. *N.Z. J. Mar. Freshwater Res.* **2004**, *38*, 255–266.
25. Gómez, I.; Ulloa, N.; Orostegui, M. *Mar. Biol.* **2005**, *148*, 231–240.
26. Gómez, I.; Ulloa, N.; Orostegui, M.; Huovinen, P. J. Phycol.. *2007* **2007**, *43*, 55–64.
27. Leinfelder, U.; Brunnenmeier, F.; Cramer, H.; Schiller, J.; Arnold, K.; Vásquez, J. A.; Zimmermann, U. *Biomaterials* **2003**, *24*, 4161–4172.
28. Shibata, T.; Kawaguchi, S.; Hama, Y.; Inagaki, M.; Yamaguchi, K.; Nakamura, T. *J. Appl. Phycol.* **2004**, *16*, 291–296.
29. Koivikko, R.; Loponen, J.; Honkanen, T.; Jormalainen, V. *J. Chem. Ecol.* **2005**, *31*, 195–212.
30. Strack, D.; Heileman, J.; Wray, V.; Dirks, H. *Phytochemistry* **1989**, *28*, 2071–2078.
31. Zimmermann, H.; Hillgärtner, M.; Manz, B.; Feilen, P.; Brunnenmeier, F.; Leinfelder, U.; Weber, M.; Cramer, H.; Schneider, S.; Hendrich, C.; Volke, F.; Zimmermann, U. *Biomaterials* **2003**, *24*, 2083–2096.
32. Kulicke, W.-M. *Chem. Ing. Tech.* **1986**, *58*, 325–327.
33. Kulicke, W.-M.; Kniewske, R.; Müller, R.-J.; Prescher, M.; Kehler, H. *Angew. Makromol. Chem.* **1986**, *142*, 29–49.
34. Bouldin, M.; Kulicke, W.-M.; Kehler, H. *Coll. Polym. Sci.* **1988**, *266*, 793–805.
35. Kulicke, W.-M.; Otto, M.; Baar, M. *Macromol. Chem. Phys.* **1993**, *194*, 751–765.
36. Kulicke, W.-M.; Kull, A. H.; Kull, W.; Thielking, H.; Engelhardt, J.; Pannek, J.-B. *Polymer* **1995**, *37*, 2723–2731.
37. Schittenhelm, N.; Kulicke, W.-M. *Macromol. Chem. Phys.* **2000**, *201*, 1976–1984.
38. Kulicke, W.-M.; Clasen, C. *Viscosimetry of Polymers and Polyelectrolytes*; Springer: Berlin, Heidelberg, New York, 2004.
39. Einstein, A. *Ann. Phys.* **1910**, *338*, 1275–1298.
40. C, Raman; Krishnan, K. *Nat. Lond.* **1928**, *121*, 501–504.
41. Debye, P. *J. Appl. Phys.* **1944**, *15*, 338–342.
42. Zimm, B. H. *J. Chem. Phys.* **1948**, *16*, 1093–1099.
43. Wyatt, P. *Anal. Chim. Acta* **1993**, *272*, 1–40.
44. Dubois, M.; Gilles, K. A.; Hamilton, J. K.; Rebers, P. A.; Smith, F. *Anal. Chem.* **1956**, *28*, 350–356.
45. Klein, J.; Kulicke, W.-M.; Hollmann, J. Chromatographie zur Bestimmung der Molmassen- und Teilchengrößenverteilung von Polymeren. In *Analytiker Taschenbuch, Bd. 19*; Springer: Heidelberg, 1998; pp 317–349.
46. Adolphi, U.; Kulicke, W.-M. *Polymer* **1997**, *38*, 1513–1519.
47. Kulicke, W.-M.; Böse, N. *Colloid. Polym. Sci.* **1984**, *262*, 197–207.
48. Kulicke, W.-M.; Clasen, C.; Lohmann, C. *Macromol. Symp.* **2005**, *223*, 151–174.
49. Roessner, D.; Kulicke, W.-M. *J. Chromatogr., A* **1994**, *687*, 249–258.
50. Wahlund, K. G.; Giddings, J. C. *Anal. Chem.* **1987**, *59*, 1332–1339.
51. Schimpf, M.; Caldwell, K.; Giddings, J. C. *Field Flow Fractionation Handbook*; Wiley & Sons: Hoboken, 2000.
52. Davis, T. A.; Llanes, F.; Volesky, B.; Diaz-Pulido, G.; McCook, L.; Mucci, A. *Appl. Biochem. Biotechnol.* **2003**, *110*, 75–90.
53. Wandrey, Ch.; Vidal, D. S. *Ann. N.Y. Acad. Sci.* **2001**, *944*, 187–198.
54. Grasdalen, H.; Larsen, B.; Smidsrød, O. *Carbohydr. Res.* **1979**, *68*, 23–31.
55. Smidsrød, O.; Haug, A. *Acta Chem. Scand.* **1968**, *22*, 797–810.
56. Mackie, W.; Noy, R.; Sellen, D. B. *Biopolymers* **1980**, *19*, 1839–1860.
57. Martinsen, A.; Skjåk-Bræk, G.; Smidsrød, O.; Zanetti, F.; Paoletti, S. *Carbohydr. Polym.* **1991**, *15*, 171–193.
58. Smidsrød, O.; Glover, R. M.; Whittington, S. G. *Carbohydr. Res.* **1973**, *27*, 107–118.
59. Vold, I. M. N.; Kristiansen, K. A.; Christensen, B. E. *Biomacromolecules* **2006**, *7*, 2136–2146.
60. Giddings, J. C. *Adv. Chromatogr.* **1982**, *20*, 217.
61. Porsch, B.; Laga, R.; Konak, C. *J. Liq. Chromatogr. Related Technol.* **2008**, *31*, 3077–3093.
62. Rousseaux, G.; De Wita, A.; Martin, A. *J. Chromatogr., A* **2007**, *1149*, 254–273.
63. Holt, C.; Mackie, W.; Sellen, D. B. *Polymer* **1976**, *17*, 1027–1034.
64. Zimmermann, U.; Klöck, G.; Federlin, K.; Hannig, K.; Kowalski, M.; Bretzel, R. G.; Horcher, A.; Entenmann, H.; Sieber, U.; Zekorn, T. *Electrophoresis* **1992**, *13*, 269–274.
65. Grasdalen, H. *Carbohydr. Res.* **1983**, *118*, 255–260.
66. Baar, A.; Kulicke, W.-M.; Szablikowski, K.; Kiesewetter, R. *Macromol. Chem. Phys.* **1994**, *195*, 1483–1492.
67. Venegas, M.; Matsuhiro, B.; Edding, M. E. *Botanica Marina* **1993**, *36*, 47–51.
68. Indergaard, M.; Skjåk-Bræk, G.; Jensen, A. *Botanica Marina* **1990**, *33*, 277–288.
69. Vold, I. M. N.; Kristiansen, K. A.; Christensen, B. E. *Biomacromolecules* **2007**, *8*, 2627.
70. Flory, P. J.; Fox, T. G. *J. Am. Chem.* **1951**, *73*, 1904.
71. Zimmermann, U.; Thürmer, F.; Jork, A.; Weber, M.; Miemietz, S.; Hillgärtner, M.; Brunnenmeier, F.; Zimmermann, H.; Westphal, I.; Fuhr, G.; Nöth, U.; Haase, A.; Steinert, A.; Hendrich, C. *Ann. N.Y. Acad. Sci.* **2001**, *944*, 199–215.